# Experimental Compton-scattering cross sections for Si and Ge

T. Paakkari and P. Suortti
*Department of Physics, University of Helsinki, SF-00170 Helsinki 17, Finland*
(Received 18 June 1973)

Compton-scattering cross sections of Si and Ge for Cu$K\alpha$ radiation are determined by direct absolute measurement of the intensity scattered from a single crystal. Parasitic components are eliminated by an evacuated specimen chamber and by combined use of a scintillation counter and a Si(Li) solid-state detector. The contribution of the thermal diffuse scattering is subtracted by a calculation based on independently determined phonon frequecies. At large scattering angles the contribution of the Compton scattering is separated directly by the Si(Li) detector. In the case of Si, a good agreement with the Waller-Hartree theory is obtained above $\sin\theta/\lambda = 0.2$ Å$^{-1}$. The experimental values for Ge are considerably larger than the theoretical ones, particularly at small scattering angles. To explain the origin of these discrepancies theoretical calculations which allow for electron binding in the Compton process and include the effects of the band structure of Ge crystal are needed.

## I. INTRODUCTION

Theoretical calculations of the Compton-scattering cross section are based on the assumption that the energy of the incident quanta is much larger than the binding energies of the electrons. In the first rigorous quantum-mechanical treatment by Waller and Hartree,[1] the cross section is obtained by subtracting the coherent part and the forbidden transitions from the total free-atom scattering cross section. The so-called impulse approximation (IA) was introduced[2] for interpretation of the measured Doppler broadening of the Compton line in terms of the one-electron wave functions. This IA theory also treats the electrons which are scattered as free rather than bound.

The theoretical understanding of the Compton process in the case of bound electrons is at present unsatisfactory. The validity of the approximations has been studied by model calculations,[3] but their nature has been too restrictive to allow conclusions about many-electron atoms in the range where the energy of the incident quanta is comparable with the binding energies of the electrons. From the practical point of view, an accurate knowledge of the Compton intensity is essential when the components of the total scattering are to be separated. This situation is encountered in most crystallographic studies, and it is the central problem in a measurement of the diffuse scattering.

There have been a few earlier attempts of direct verification of the theoretical predictions, e.g., Walker,[4] and subsidiary measurements of the Compton intensity have been made in connection with diffuse-scattering experiments, e.g., Buyers and Smith.[5] The general conclusion of these studies has been that the Waller-Hartree values, as calculated by Freeman,[6] are valid also at the wavelengths used in crystallography. In this paper we report measurements on Si and Ge single crystals, made with improved techniques. Si and Ge were selected since they represented two essentially different cases in the Compton scattering. Practical considerations also played a decisive role in our choice: Cu$K\alpha$ radiation does not excite interfering fluorescence, and the lattice dynamics of the two crystals are accurately known.

## II. INTENSITY OF INELASTIC SCATTERING

Consider an arrangement where a monochromatic x-ray beam hits a totally absorbing crystalline specimen in a symmetrical-reflection geometry, i.e., the incident and detected rays make equal angles $\theta$ with the flat specimen surface. In addition to the elastic or Bragg scattering, the scattered radiation consists of the inelastic Compton and (almost elastic) thermal diffuse scattering (TDS). If the incident x-ray photon flux is $n_0$, the flux of the detected quanta is

$$n = n_0 \Omega M_0 K_{\text{pol}} \left( \frac{(d\sigma/d\Omega)_C}{\mu_0 + \mu_C} + \frac{(d\sigma/d\Omega)_{\text{TDS}}}{2\mu_0} \right), \qquad (1)$$

where $\Omega$ is the solid angle subtended by the receiving slit and $M_0$ is the number of atoms per unit volume. The linear absorption coefficients for the unmodified and Compton-modified scattering are denoted by $\mu_0$ and $\mu_C$, respectively. The scattering cross sections per atom are, for the Compton process, $(d\sigma/d\Omega)_C$, and for the TDS, $(d\sigma/d\Omega)_{\text{TDS}}$. $K_{\text{pol}}$ is the ratio of the polarization factor of the scattered radiation to that of the monochromated primary beam. In the present case the kinematic approximation is valid, and

$$K_{\text{pol}} = (1 + K\cos^2 2\theta)/(1 + K), \qquad (2)$$

where $K$ is the polarization ratio of the primary beam, $I(\pi)/I(\sigma)$.

In the following, the theoretical calculation of

$(d\sigma/d\Omega)_C$ and $(d\sigma/d\Omega)_{TDS}$ is considered. Numerical values for the TDS contribution are evaluated and subtracted from the total experimental-scattering cross section. The remainder is then compared with the theoretical prediction for $(d\sigma/d\Omega)_C$. The experimental details of determining $n$, $n_0$, $\Omega$, and $K_{pol}$ are discussed in a separate section.

## III. COMPTON CROSS SECTION

The scattering cross section of one free electron, initially at rest in the laboratory frame, is given by the well-known Klein-Nishina formula,[7]

$$\frac{d\sigma}{d\Omega} = r_0^2\left(\frac{w_2^0}{w_1}\right)^3\left(\frac{w_1}{w_2^0} + \frac{w_2^0}{w_1} - 2 + 4(\vec{e}_1\cdot\vec{e}_2)^2\right) f_C^2 , \quad (3)$$

where $r_0 = e^2/mc^2$ is the classical electron radius and $f_C$ is the incoherent scattering factor, while $w_1$ and $w_2^0$ are the initial and final photon energies, respectively (the superscript on $w_2$ indicates the special case of the electron initially at rest). The (unit) polarization vectors of the incident and scattered waves are denoted by $\vec{e}_1$ and $\vec{e}_2$, respectively. As indicated in Eq. (2), the polarization factor $(\vec{e}_1\cdot\vec{e}_2)^2 = \frac{1}{2}(1 + K\cos^2 2\theta)$. With this notation,

$$\frac{w_2^0}{w_1} = \left(1 + \frac{w_1}{mc^2}(1 - \cos 2\theta)\right)^{-1} . \quad (4)$$

Equation (3) can be extended to the $Z$-electron system of a free atom by considering the expression for $f_C^2$. The nonrelativistic situation in the case of large $w_1$ is summarized in the Waller-Hartree expression,[1]

$$f_{WH}^2 = Z - \sum_{j=1}^{Z} |f_{jj}|^2 - \sum_j \sum_{k\neq j} |f_{jk}|^2 , \quad (5)$$

where

$$f_{jk} = \int \psi_j^* \psi_k e^{i\vec{Q}\cdot\vec{r}}\, d^3r .$$

Here $\vec{Q}$ is the x-ray scattering vector of magnitude $4\pi\sin\theta/\lambda$, and the $\psi$'s are the appropriate one-electron wave functions. The third term in Eq. (5) excludes the forbidden transitions from the scattering cross section. Numerical values based on Hartree-Fock wave functions have been published by Freeman.[6] In the nonrelativistic approximation $w_1 \ll mc^2$ and $w_1/w_2^0 + w_2^0/w_1 \approx 2$ ($\leqq 2.000\,43$ in the present case of $w_1 = 8$ keV) in Eq. (3). Because the counter records the flux of quanta instead of the flux of energy, Eq. (3) should be multiplied by $w_1/w_2^0$. Furthermore, since the polarization factor is included in Eq. (1), it is dropped from the following expression for the Compton-scattering cross section in the Waller-Hartree approximation

$$\left(\frac{d\sigma}{d\Omega}\right)_{WH} = \left(\frac{d\sigma}{d\Omega}\right)_{Th} f_{WH}^2 \quad (\vec{e}_1\cdot\vec{e}_2)^2 , \quad (6)$$

where

$$\left(\frac{d\sigma}{d\Omega}\right)_{Th} = r_0^2\left(\frac{w_2^0}{w_1}\right)^2 (\vec{e}_1\cdot\vec{e}_2)^2 \quad (7)$$

is the nonrelativistic Thompson cross section.

In the impulse approximation the one-dimensional Compton profile, $J_j(p_Q)$, for each one-electron orbital $j$ is obtained from the ground-state momentum wave function $\chi_j(\vec{p})$ by

$$J_j(p_Q) = 2\pi\int_{|p_Q|}^{\infty} |\chi_j(\vec{p})|^2 p\, dp . \quad (8)$$

The $\chi_j(\vec{p})$'s, which are the Fourier transforms of the direct space wave functions, are normalized by

$$4\pi\int_0^{\infty} |\chi_j(\vec{p})|^2 p^2\, dp = 1 . \quad (9)$$

$J_j(p_Q)$ is symmetrical about $p_Q = 0$, which corresponds to an energy of $w_2^0$ of the scattered quanta. It is now possible to express the cross section in the IA for the one-electron orbital $j$ as an integral over the Compton profile[8]

$$\left(\frac{d\sigma}{d\Omega}\right)_{IA}^{j} = r_0^2\int_{|\epsilon_j|}^{w_1} \frac{w_2}{w_1}\frac{m}{|\vec{Q}|} J_j(p_Q)\, dw , \quad (10)$$

where the polarization factor $(\vec{e}_1\cdot\vec{e}_2)^2$ is dropped. Equation (10) is valid when the energy transfer, $w = w_1 - w_2$, is small ($w \ll mc^2$), and in that case the relationship between $p_Q$ and $w$ is given by

$$p_Q = mw/|\vec{Q}| - \tfrac{1}{2}|\vec{Q}| . \quad (11)$$

Although Eq. (8) was derived for electrons whose binding energy is negligible when compared with the energy transferred by the photon, an allowance is made for the electron binding in Eq. (10). The cross section $(d\sigma/d\Omega)_{IA}^{j}$ is integrated from the one-electron binding energy $|\epsilon_j|$ to an upper limit of the incident photon energy $w_1$. The final cross section in the IA is obtained by summing over all one-electron orbitals,

$$\left(\frac{d\sigma}{d\Omega}\right)_{IA} = \sum_{j=1}^{Z}\left(\frac{d\sigma}{d\Omega}\right)_{IA}^{j} . \quad (12)$$

Each of the electron orbitals is normalized by

$$\int_{-\infty}^{\infty} J_j(p_Q)\, dp_Q = 1 , \quad (13)$$

in accordance with Eqs. (8) and (1).

The values of $(d\sigma/d\Omega)_{IA}$ in electron units ($r_0 = 1$) are tabulated by Currat, DeCicco, and Weiss[8] for several elements and for Mo$K\alpha$ and Cu$K\alpha$ radiation. While the normalization (13) is justifiable at large values of $Q$, it is not valid when $Q$ is small. Correspondingly, several authors[8–10] have preferred normalization according to Waller-Hartree theory

$$\int_{-\infty}^{\infty} J_j(p_Q)\, dp_Q = 1 - f_{jj}^2 , \quad (14)$$

in order to take the contribution of the coherent scattering into account. This considered in greater detail when the results on Ge are discussed.

## IV. TDS CROSS SECTION

One reason for selecting Ge and Si as objects of measurement was that the intensity of the thermal diffuse scattering is relatively low in both cases, and that it can be calculated reliably from the dispersion curves determined by neutron diffraction.

### A. One-phonon TDS

Following Cochran,[11] the one-phonon scattering cross section per primitive unit cell containing $n$ atoms can be written as

$$\left(\frac{d\sigma}{d\Omega}\right)^{(1)} = r_0^2 \frac{Q^2}{m} \sum_{j=1}^{3n} \frac{E_j(\vec{q})}{\omega_j^2(\vec{q})} |G_j^{(1)}(\vec{Q})|^2 ,$$

$$QG_j^{(1)}(\vec{Q}) = \vec{Q} \cdot \sum_{k=1}^{n} \vec{U}_{j,k}^0(\vec{q}) f_k(\vec{Q}) e^{-M_k} e^{i\vec{B}\cdot\vec{r}_k} , \quad (15)$$

where $E_j(\vec{q})$ is the energy of the mode of angular frequency $\omega_j(\vec{q})$, and $\vec{B}$ is a vector of the reciprocal lattice. The vector $\vec{r}_k$ defines the equilibrium position of the $k$th atom within its cell, for which $f_k(\vec{Q})$ is the scattering factor, and $e^{-M_k}$ is the Debye-Waller factor. The normalized wave amplitudes $\vec{U}_{j,k}^0(\vec{q})$ are defined by

$$\sum_{k=1}^{n} m_k |\vec{U}_{j,k}^0(\vec{q})|^2 = \sum_{k=1}^{n} m_k = m , \quad (16)$$

where $m_k$ is the mass of the $k$th atom.

The diamond-type lattice of Si and Ge is composed of two equivalent interpenetrating face-centered cubic lattices. The positions of the two atoms of a primitive unit cell are

$$\vec{r}_1 = a(0,0,0) \text{ and } \vec{r}_2 = a(\tfrac{1}{4},\tfrac{1}{4},\tfrac{1}{4}) ,$$

where $a$ is the lattice constant. Accordingly, there are three acoustic- and three optical-phonon branches. Equation (15) takes a particularly simple form when the scattering vector is along a symmetry direction of the crystal. In that case only the longitudinal phonons contribute to the one-phonon TDS. When the corresponding wave amplitudes are substituted, the following "structure factor" for the one-phonon TDS is obtained:

$$G_j^{(1)}(\vec{Q}) = f(\vec{Q}) e^{-M}(1 \pm e^{i\vec{B}\cdot\vec{r}_2} e^{i\varphi_2(\vec{q})}) . \quad (17)$$

The upper sign corresponds to the acoustic branch and the lower one to the optical branch. The phase of motion of atom (2), relative to atom (1), is denoted by $\varphi_2(\vec{q})$. In the present case the measurements were made in the vicinity of the Brillouin zone boundaries in the $[h,h,h]$ direction, or at

$$(h,k,l) = (2p+1)(\tfrac{1}{2},\tfrac{1}{2},\tfrac{1}{2}) , \quad (18)$$

where $p$ is an integer. The corresponding values of $\varphi_2(\vec{q})$ are $\pm\frac{3}{4}\pi$ for $q = \pm q_m$, respectively; $q_m$ is the maximum wave vector. At these points Eq. (15) reduces to

$$\left(\frac{d\sigma}{d\Omega}\right)^{(1)} = r_0^2 \frac{f^2 e^{-2M}}{2m} Q^2 \left\{ \left(\frac{E(q_m)}{\omega^2(q_m)}\right)_{LA} \left[\left(\frac{\sqrt{2}\mp 1}{\sqrt{2}}\right)^2 + \frac{1}{2}\right] + \left(\frac{E(q_m)}{\omega^2(q_m)}\right)_{LO} \left[\left(\frac{\sqrt{2}\pm 1}{\sqrt{2}}\right)^2 + \frac{1}{2}\right] \right\} , \quad (19)$$

where the upper sign corresponds to the case $p = 1, 2$ and the lower one to $p = 0, 3$.

### B. Two-phonon TDS

The two-phonon intensity at $\vec{Q}$ is a sum of the contributions from the phonon pairs $(\vec{q}', \vec{q} - \vec{q}')$ that satisfy the diffraction condition $\vec{B} = \vec{Q} + \vec{q}' + (\vec{q} - \vec{q}')$. The scattering cross section per primitive unit cell is

$$\left(\frac{d\sigma}{d\Omega}\right)^{(2)} = \frac{r_0^2}{2Nm^2} \sum_{i,j=1}^{3n} \sum_{\vec{q}'} \frac{E_j(\vec{q}')E_i(\vec{q}-\vec{q}')}{\omega_j^2(\vec{q}')\omega_i^2(\vec{q}-\vec{q}')} |G_{ij}^{(2)}(\vec{Q})|^2 ,$$

$$G_{ij}^{(2)}(\vec{Q}) = \sum_{k=1}^{n} f_k(\vec{Q}) e^{-M_k} \exp\{[i\vec{B}\cdot\vec{r}_k][\vec{Q}\cdot\vec{U}_{j,k}^0(\vec{q}')] \times [\vec{Q}\cdot\vec{U}_{i,k}^0(\vec{q}-\vec{q}')]\} , \quad (20)$$

where $N$ is the number of unit cells in the crystal. The numerical values were calculated by an approximate method, which is essentially the procedure described by Walker[12] as generalized to crystals with more than one atom per primitive unit cell. The contributions of the optical modes were calculated by assigning constant frequencies $\omega_{LO}$ and $\omega_{TO}$ to the respective phonon branches. The actual formulas are very cumbersome, and the details of the calculation are given elsewhere.[13]

Lomer[14] has studied the relative importance of one-phonon and two-phonon scattering processes in the total TDS intensity. On the basis of this calculation it was concluded that in the present case the higher-order contribution was negligible when compared with the uncertainties in $(d\sigma/d\Omega)^{(1)}$ and $(d\sigma/d\Omega)^{(2)}$, and it was accordingly ignored.

The relevant parameters used in evaluating the TDS cross sections are given in Table I. They are based mainly on the neutron diffraction measurements by Brockhouse and Iyengar,[18] and Dolling,[19] and on a scattering factor measurement by Jennings.[20] As to Ge, a recent measurement by Nilsson and Nelin[21] at 80 °K suggests that somewhat narrower bounds can be assigned to the experimental $\omega$'s than those given by Brockhouse and Iyengar. A slightly lower value ($3.90\times10^{13}$ sec$^{-1}$) was adopted for $\omega_{LA}(q_m)$ in order to allow for the effect of a relatively wide receiving slit. The resulting cross sections, $(d\sigma/d\Omega)_{TDS}$, in electron units are given in Table II.

## V. EXPERIMENTAL

Intensity measurements were made on large Ge and Si single crystals that were cut perpendicular

TABLE I. Parameters used in the evaluation of the TDS cross sections for Si and Ge.

| | | Si | Ge |
|---|---|---|---|
| Lattice parameter | (Å) | 5.4310 | 5.6577 |
| Atomic weight | | 28.086 | 72.59 |
| $B(M=B\sin^2\theta/\lambda^2)$ | (Å$^2$) | 0.446 | 0.562 |
| $f$ | | Ref. 15 | Ref. 15 |
| $\Delta f'$ | | 0.21 | −1.04 |
| $\mu_{\text{lin}}$[a] | (1/cm) | 151.0 | 357.0 |
| $\omega_{\text{LA}}(q_m)$ | ($10^{13}$ sec$^{-1}$) | 7.15 | 3.90 |
| $\omega_{\text{LO}}(q_m)$ | ($10^{13}$ sec$^{-1}$) | 7.90 | 4.65 |
| $\omega_{\text{TO}}$ | ($10^{13}$ sec$^{-1}$) | 9.47 | 5.40 |
| $\omega_{\text{LO}}$ | ($10^{13}$ sec$^{-1}$) | 9.10 | 5.02 |
| $V_{\text{TA}}$ | (km/h) | 5.20 | 3.00 |
| $V_{\text{LA}}$ | (km/h) | 8.90 | 5.50 |

[a]From Ref. 16 as corrected for scattering (Ref. 17).

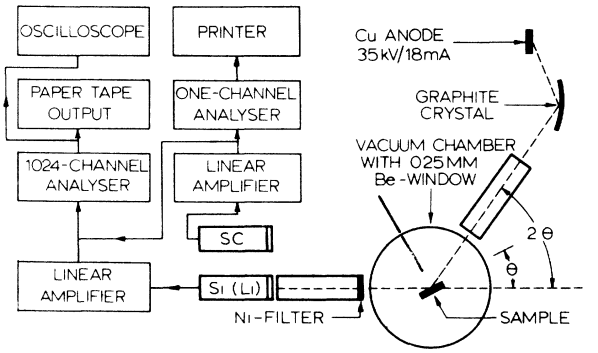


FIG. 1. Schematic drawing of the experimental arrangement.

to the $[h,h,h]$ direction. The points of measurement were selected around $(2p+1)(\frac{1}{2},\frac{1}{2},\frac{1}{2})$ in reciprocal space, with $p=0$, 1, 2, and 3. The experimental arrangement is shown schematically in Fig. 1. The Cu-anode x-ray tube was operated at 35 kV, 18 mA, and $K\alpha$ radiation was selected by a singly-bent graphite monochromator. The specimen was enclosed in a vacuum chamber, and the collimators and shields were arranged in such a way as to prevent parasitic scattering from rays entering the receiving slit. The angular width of the slit was determined by scanning it across a pinhole x-ray beam; the slit length was measured by rotating the slit through 90°. The effects of the finite size of the receiving slit were corrected according to Suortti and Jennings.[22]

A block diagram of the measuring system is also shown in Fig. 1. The actual determinations of $n_0$ and $n$ [Eq. (1)] were made by a scintillation counter (SC) connected to a single-channel-analyzer system (SCA). The respective pulse-height distribution was recorded simultaneously through a multichannel analyzer (MCA). The actual energy distribution of the received radiation was measured by a Si(Li) detector connected to the MCA. In the case of Ge, this inspection revealed the presence of strong Ge$K$ fluorescence in the detected beam, which had been excited by the $\frac{1}{2}\lambda$, $\frac{1}{3}\lambda$, and $\frac{1}{4}\lambda$ components of the primary beam. The fluorescence was reduced to a tolerable level by placing a Ni absorber in front of the diffracted beam tunnel. The reflections of the $\frac{1}{2}\lambda$ component at the zone boundaries were avoided by making the measurements at several off-reflection positions on both sides of the boundary; the actual value was determined by interpolation. A comparison between the energy distributions as recorded by the SC and the Si(Li) detector made it possible to subtract the extraneous counts. The corrections were −2.8%, −0.7%, −0.6%, and −0.6% for $p=0$, 1, 2, and 3, respectively.

The power of the primary beam was measured by the SC and SCA, and the beam was attenuated by calibrated Ni foils. The dead time was determined by the method suggested by Chipman.[23] It was noted that the actual, total counting rate for a strongly attenuated beam was determined largely by the $\frac{1}{3}\lambda$ and $\frac{1}{4}\lambda$ harmonics for which the Ni foils were relatively transparent.

At the highest point of measurement, $p=3$, it was possible to separate the Compton intensity experimentally by using the Si(Li) detector. A statistically good measurement of the pulse-height distribution of the combined Compton plus TDS scattering was made. The response of the Si(Li) detector to the practically monoenergetic TDS was

TABLE II. The experimental total cross sections and the calculated one-phonon and two-phonon TDS cross sections for Si and Ge, given in electron units and for one atom.

| | Si | | | | Ge | | | |
|---|---|---|---|---|---|---|---|---|
| | $\left(\frac{d\sigma}{d\Omega}\right)^{(1)}$ | $\left(\frac{d\sigma}{d\Omega}\right)^{(2)}$ | $\left(\frac{d\sigma}{d\Omega}\right)_{\text{TDS}}$ | Total | $\left(\frac{d\sigma}{d\Omega}\right)^{(1)}$ | $\left(\frac{d\sigma}{d\Omega}\right)^{(2)}$ | $\left(\frac{d\sigma}{d\Omega}\right)_{\text{TDS}}$ | Total |
| $(\frac{1}{2},\frac{1}{2},\frac{1}{2})$ | 0.32 | 0.00 | 0.32 | 1.28 | 1.46 | 0.01 | 1.47 | 3.98 |
| $(\frac{3}{2},\frac{3}{2},\frac{3}{2})$ | 1.52 | 0.06 | 1.58 | 6.37 | 10.02 | 0.65 | 10.67 | 17.54 |
| $(\frac{5}{2},\frac{5}{2},\frac{5}{2})$ | 2.53 | 0.30 | 2.83 | 9.55 | 15.56 | 2.89 | 18.45 | 28.90 |
| $(\frac{7}{2},\frac{7}{2},\frac{7}{2})$ | 2.46 | 0.41 | 2.87 | 10.79 | 12.24 | 3.78 | 16.02 | 28.22 |

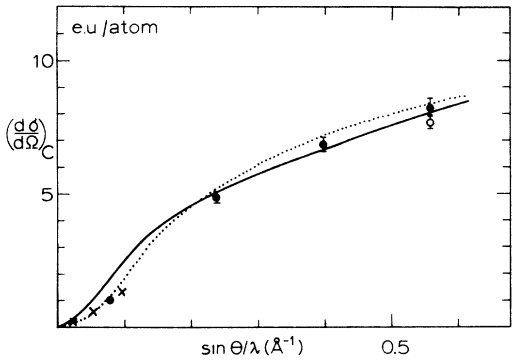


FIG. 2. Comparison of the experimental $(d\sigma/d\Omega)_C$ (circles) for Si with those in the Waller-Hartree theory (solid curve). The values $f^2_{WH}$, as given by Freeman (Ref. 6), have been multiplied by $(\omega_2^0/\omega_1)^2$. The dotted curve gives the IA values calculated by Currat *et al.* (Ref. 8). The open circle corresponds to the result of an experimental separation of the Compton scattering by the Si (Li) detector. Earlier results by Weinberg (Ref. 24) are indicated by crosses. The experimental error, which is mainly due to the assessed accuracy of the theoretical or experimental separation of the contribution of the TDS is indicated by error bars or by the size of the circle.

determined by measuring air scattering of the primary radiation at a low scattering angle. The width of the resolution function [full width at half-maximum (FWHM)] was 258 eV. As the Compton shift at $2\theta = 111°$ (for Ge) was only 169 eV, the two distributions overlapped considerably. Successive multiples of a function with the shape of the TDS

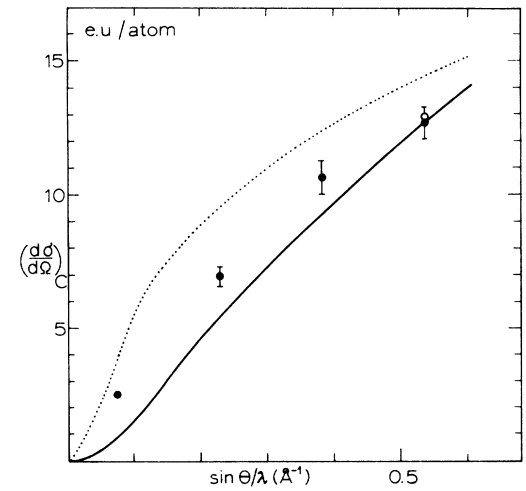


FIG. 3. Experimental results for Ge. The dotted curve gives the IA values calculated by Currat *et al.* (Ref. 8). With the Waller-Hartree normalization [Eq. (14)], the IA values coincide with the Waller-Hartree curve (solid line). For an explanation of further details of the figure, see the caption to Fig. 2.

contribution were subtracted from the measured total until the background level was reached but not exceeded. The resulting shares of the Compton scattering are (67 ± 2)% and (44 ± 2)% for Si and Ge, respectively. As seen in Figs. 2 and 3, these values are in excellent agreement with the cross section obtained by subtracting the calculated TDS contribution.

## VI. RESULTS AND DISCUSSION

The experimental Compton-scattering cross sections for Si and Ge are presented in Figs. 2 and 3 together with theoretical curves. Table III gives the binding energies of the electrons and the average energy transfer to an electron at the various scattering angles. In the case of Si, $w_1 - w_2^0$ is comparable to the binding energy is most cases, and the measurement agrees with the Waller-Hartree calculation within experimental error, when $\sin\theta/\lambda > 0.2$ Å$^{-1}$. At low $\sin\theta/\lambda$ the experimental result (0.96 e.u.) is about 50% less than the Waller-Hartree value and is in good agreement with an earlier result (1.0 e.u.) by Weinberg.[24] The $K$ electrons of Ge are not excited at all, and the binding energies of the eight $L$ electrons are much larger than $w_1 - w_2^0$; for the rest of the electrons, the situation is similar to that in Si. The experimental points lie between the two theoretical curves. However, the large values of the IA calculation by Currat, DeCicco, and Weiss,[8] which exceed the Waller-Hartree figures by as much as a factor of 3, originate in adopting the normalization condition of Eq. (13), which is not valid at small values of $\sin\theta/\lambda$. When the weights given by Eq. (14), which takes account of the coherent scattering, are used, the IA curve coincides with the Waller-Hartree values.

The fact that the experimental values of $(d\sigma/d\Omega)_C$ for Ge are considerably higher than those predicted by the Waller-Hartree theory, particularly at small values of $\vec{Q}$, is interesting. A similar trend was observed by Eisenberger and Platzman[3] when they carried out an exact calculation for hydrogenlike

TABLE III. The binding energies of the electrons in free Si and Ge atoms, and the values of the average transfer of energy (in eV) to an electron at the various points of measurement. The energy of the incident photons in 8.04 keV.

| | Si | | | | Ge | | | |
|---|---|---|---|---|---|---|---|---|
| $\epsilon_K$ | 1839 | | | | 11 103 | | | |
| $\epsilon_L$ | 149 – 99 | | | | 1414 – 1217 | | | |
| $\epsilon_M$ | ≈ 7 | | | | 180 – 29 | | | |
| $\epsilon_N$ | | | | | ≈ 3 | | | |
| $p$ | 0 | 1 | 2 | 3 | 0 | 1 | 2 | 3 |
| $w_1 - w_2^0$ | 4 | 34 | 94 | 183 | 4 | 32 | 87 | 169 |

free atoms. However, the main reason for the departure from the Waller-Hartree theory is presumably that the theoretical calculations are for free atoms rather than for atoms in a solid. At low $\vec{Q}$ the main contribution to $(d\sigma/d\Omega)_C$ comes from the valence electrons, whose energies are affected by the crystal field. At $(h,k,l)=(\frac{1}{2},\frac{1}{2},\frac{1}{2})$ the average energy transfer to an electron is about 4 eV, which is considerably larger than the minimum energy gap of 0.7 eV between the valence and conduction bands of Ge. This explains qualitatively the observed high value of $(d\sigma/d\Omega)_C = 2.51$ at this point.

The present findings suggest that the Waller-Hartree values are valid when the energy transfer $w_1 - w_2^0$ is comparable with the binding energies of the majority of the electrons. This seems to apply even when $\epsilon_L = 4(w_1 - w_2^0)$, which is the case at $(\frac{3}{2},\frac{3}{2},\frac{3}{2})$ in Si. When the energy transfer is very small, the solid-state effects become important and the theoretical calculations should include the band structure of the crystal. Apart from providing a better understanding of the Compton process at small energy transfer, this would be of importance to crystallographic studies. For, let us suppose that the TDS intensity is to be determined in a case similar to that at $(\frac{1}{2},\frac{1}{2},\frac{1}{2})$ in Ge. Direct subtraction of the Waller-Hartree value of 1.0 from the total of 4.0 would yield a value of 3.0 for $(d\sigma/d\Omega)_{TDS}$, whereas the observed value is 1.5.


[1] I. Waller and D. R. Hartree, Proc. Roy. Soc. A 124, 119 (1929).
[2] P. M. Platzman and N. Tzoar, Phys. Rev. 139, A410 (1965).
[3] P. Eisenberger and P. Platzman, Phys. Rev. A 2, 415 (1970).
[4] C. B. Walker, Phys. Rev. 103, 558 (1956).
[5] W. J. L. Buyers and T. Smith, Phys. Rev. 150, 758 (1966).
[6] A. J. Freeman, Acta Crystallogr. 12, 929 (1959).
[7] O. Klein and Y. Nishina, Z. Phys. 52, 853 (1929).
[8] R. Currat, P. D. DeCicco, and R. J. Weiss, Phys. Rev. B 4, 4256 (1971).
[9] W. C. Phillips and R. J. Weiss, Phys. Rev. 171, 790 (1968).
[10] R. Currat, P. D. DeCicco, and R. Kaplow, Phys. Rev. B 3, 243 (1971).
[11] W. Cochran, Rep. Prog. Phys. 26, 1 (1963).
[12] C. B. Walker, Phys. Rev. 103, 547 (1956).
[13] P. Suortti, Rep. Ser. Phys., Univ. Helsinki, No. 53 (1973).
[14] T. R. Lomer, Proc. Phys. Soc. 89, 135 (1966).
[15] *International Tables for X-ray Crystallography* (Kynoch, Birmingham, 1962), Vol. III, pp. 202–205.
[16] J. H. Hubbell, W. H. McMaster, N. K. Del Grande, and J. H. Mallett (unpublished).
[17] J. J. DeMarco and P. Suortti, Phys. Rev. B 4, 1028 (1971).
[18] B. N. Brockhouse and P. K. Iyengar, Phys. Rev. 111, 747 (1958).
[19] G. Dolling, in *Inelastic Scattering of Neutrons in Solids and Liquids* (International Atomic Energy Agency, Vienna, 1963), Vol. II, p. 37; in *Inelastic Scattering of Neutrons* (International Atomic Energy Agency), Vol. I, p. 249.
[20] L. D. Jennings, J. Appl. Phys. 40, 5038 (1969).
[21] G. Nilsson and G. Nelin, Phys. Rev. B 3, 364 (1971).
[22] P. Suortti and L. D. Jennings, J. Appl. Crystallogr. 4, 37 (1971).
[23] D. R. Chipman, Acta Crystallogr. A 25, 209 (1969).
[24] D. L. Weinberg, Phys. Rev. 134, A1016 (1964).